A simple ligand that selectively targets CUG trinucleotide repeats and inhibits MBNL protein binding

Jonathan F. Arambula, Sreenivasa Rao Ramisetty, Anne M. Baranger[1], and Steven C. Zimmerman[1]

Department of Chemistry, University of Illinois, 600 South Mathews Avenue, Urbana, IL 61801

Edited by Gregory A. Petsko, Brandeis University, Waltham, MA, and approved July 16, 2009 (received for review February 19, 2009)

This work describes the rational design, synthesis, and study of a ligand that selectively complexes CUG repeats in RNA (and CTG repeats in DNA) with high nanomolar affinity. This sequence is considered a causative agent of myotonic dystrophy type 1 (DM1) because of its ability to sequester muscleblind-like (MBNL) proteins. Ligand 1 was synthesized in two steps from commercially available compounds, and its binding to CTG and CUG repeats in oligonucleotides studied. Isothermal titration calorimetry studies of 1 with various sequences showed a preference toward the T-T mismatch (K_d of 390 ± 80 nM) with a 13-, 169-, and 85-fold reduction in affinity toward single C-C, A-A, and G-G mismatches, respectively. Binding and Job analysis of 1 to multiple CTG step sequences revealed high affinity binding to every other T-T mismatch with negative cooperativity for proximal T-T mismatches. The affinity of 1 for a $(CUG)_4$ step provided a K_d of 430 nM with a binding stoichiometry of 1:1. The preference for the U-U in RNA was maintained with a 6-, >143-, and >143-fold reduction in affinity toward single C-C, A-A, and G-G mismatches, respectively. Ligand 1 destabilized the complexes formed between MBNL1N and $(CUG)_4$ and $(CUG)_{12}$ with IC_{50} values of 52 ± 20 μM and 46 ± 7 μM, respectively, and K_i values of 6 ± 2 μM and 7 ± 1 μM, respectively. These values were only minimally altered by the addition of competitor tRNA. Ligand 1 does not destabilize the unrelated RNA-protein complexes the U1A-SL2 RNA complex and the Sex lethal-*tra* RNA complex. Thus, ligand 1 selectively destabilizes the MBNL1N-poly(CUG) complex.

inhibition | MBNL1 | molecular recognition | myotonic dystrophy | RNA

Myotonic dystrophy type 1 (DM1) is the most common form of muscular dystrophy affecting about 1 in 8,000 people (1). DM1 is a trinucleotide repeat expansion disorder (TREDs) with $(CTG)_n$ step sequences aberrantly expanded in the 3′-untranslated region of the *DMPK* gene (2). At the RNA level, the *DMPK* transcript sequesters splicing regulator proteins, in particular muscleblind-like (MBNL) proteins, which results in incorrect splicing of a number of premRNAs, and this gain-of-function is the direct cause of DM1 (3). Indeed, it has been suggested that one therapeutic strategy would employ a drug that binds to CUG repeats, thereby freeing MBNL to regulate splicing of its pre-mRNA targets (4). Alternatively, binding looped out $(CTG)_n$ repeats may inhibit transcription of the expanded region or even reduce the expansion during repair or replication (2, 5).

In rationally developing a ligand to target the CUG or CTG repeat, the weakly paired U-U or T-T mismatch presents an obvious opportunity for recognition by hydrogen bonding. Although there are small molecules capable of hydrogen bond-mediated, selective recognition of the G-G (6), C-C (7), or A-A (8) mismatch, there is currently no known, high affinity binder that is selective for T-T or U-U mismatches. In fact, there have been very few ligands found to recognize CUG or CTG repeat sequences. Actinomycin D has been reported to bind $(CTG)_n$ repeats (9), while a macrocyclic diacridine has been shown to bind mismatches containing a T with low specificity (10). A combinatorial screening approach was used to identify peptide ligands that bind to CUG repeat sequences with modest 5- to 10-fold selectivity over duplex structures (11). These ligands may also be limited by their relatively high molecular weights and peptidic structure. Herein we report that ligand **1**, a simple triaminotriazine-acridine conjugate designed to hydrogen bond to both U's or T's in the U-U or T-T mismatch, selectively binds CTG and CUG repeats with high nanomolar affinity and inhibits the binding of a protein comprised of the RNA binding region of MBNL1 (MBNL1N, amino acids 1–272) to $(CUG)_4$ and $(CUG)_{12}$ RNAs with low micromolar K_i values in the presence of competitor tRNA.

Results and Discussion

The X-ray crystal structure of a short (CUG) sequence shows that it adopts a duplex structure that is very similar to A-form RNA, except at the U-U mismatches where the base-pairing is not optimal (4). Using this information, ligand **1** was designed with a well-known acridine DNA intercalator and a triaminotriazine unit to recognize T-T (U-U) through Janus-wedge (12, 13) hydrogen bonding (Fig. 1). Thus, the two edges of the triazine heterocycle have the potential to form simultaneously a full set of hydrogen bonds with the poorly paired thymine or uracil bases. By analogy with nucleobase-acridine conjugates (14), stacking of the triaminotriazine and acridine units should decrease nonspecific, intercalative binding to duplex DNA and RNA. Although 9-aminoacridine derivatives bind in the minor groove, molecular modeling using MOE suggested that ligand **1** could target CTG and CUG through either minor or major grooves as a "stacked intercalator."

Triaminotriazine-acridine conjugates **1**–**4** and control compounds **5**–**6** were prepared in two steps from commercially available starting materials. A qualitative structure-function relationship was established by thermal denaturation studies of DNA oligonucleotides containing two CTG steps (Fig. 2). Ligand **1** provided the greatest stabilization with a ΔT_m of + 4.5 °C, whereas conjugates of linker lengths 3, 8, and 12 displayed lower stabilizations of +1, +1, and 0 °C, respectively. A much higher ΔT_m of +16 °C was observed with **1** and analogous 8-mers (see *SI Appendix*). The triaminotriazine unit appears to contribute significantly to the binding as no stabilization was observed with **5** and **6**. Importantly, no stabilization of a normal duplex (dGCGCAGCCAG) by **1** was observed.

Author contributions: J.F.A., S.R.R., A.M.B., and S.C.Z. designed research; J.F.A. and S.R.R. performed research; J.F.A., S.R.R., A.M.B., and S.C.Z. analyzed data; and J.F.A., A.M.B., and S.C.Z. wrote the paper.

The authors declare no conflict of interest.

This article is a PNAS Direct Submission.

[1]To whom correspondence may be addressed. E-mail: baranger@illinois.edu or sczimmer@illinois.edu.

This article contains supporting information online at www.pnas.org/cgi/content/full/0901824106/DCSupplemental.

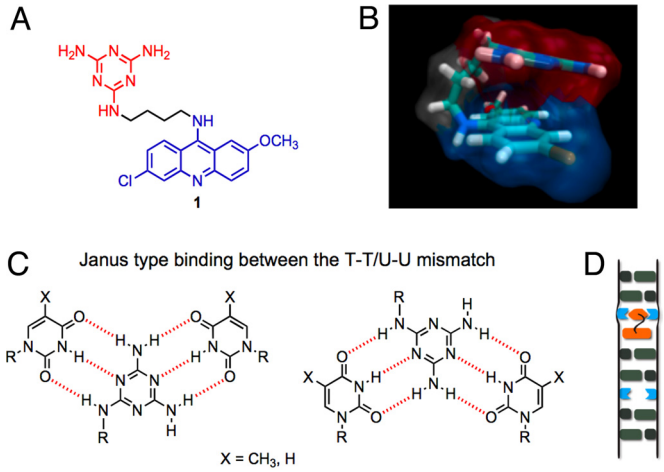

Fig. 1. (*A*) Triaminotriazine-acridine conjugate **1** designed for selective recognition of T-T and U-U mismatches. (*B*) Modeling of stacked ligand by MOE and rendering by VMD. (*C*) Proposed Janus-Wedge type binding of triaminotriazine to the T-T/U-U mismatch through minor and major grooves. (*D*) One possible binding mode of the ''stacked intercalator'' to the mismatch. See *SI Appendix* for other potential binding modes. Note that **1** will bind oligonucleotides in its protonated form.

The affinity and selectivity of **1** for T-T vs. C-C, A-A, and G-G mismatches was studied using isothermal titration calorimetry (ITC) with DNA 10-mers A–D (Fig. 3). Ligand **1** bound strand A (T-T mismatch) with a K_d of 390 ± 80 nM. The high affinity of **1** for strand A was confirmed by fluorescence titration and a 1:1 stoichiometry was shown by Job analysis. Ligand **1** bound with 13-, 169-, and 85-fold lower affinity to the C-C (B), A-A (C), and G-G (D) mismatches, respectively (Table 1). The comparatively moderate binding of **1** to the C-C mismatch in B (K_d of 5.0 ± 0.2 μM) may suggest that the binding selectivity is for pyrimidine mismatch which have a higher propensity toward an extrahelical structure (15). Alternatively, it is possible for the triaminotriazine unit to form four hydrogen bonds with the C-C

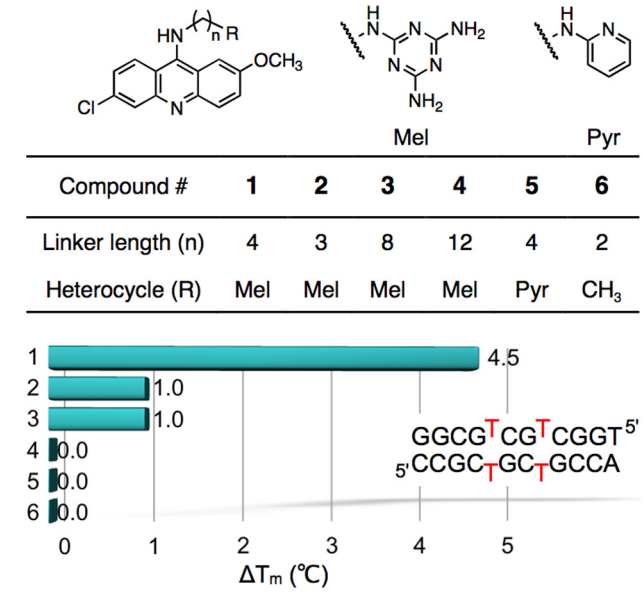

Fig. 2. Thermal denaturation studies of **1**–**6** with a DNA duplex containing two CTG steps. Graphical summary of stabilization increase of DNA in presence of the ligand. [DNA] = 12 μM duplex, [Ligand] = 24 μM, [Mops] = 20 mM, pH 7.0, [NaCl] = 300 mM, [EDTA] = 1 mM.

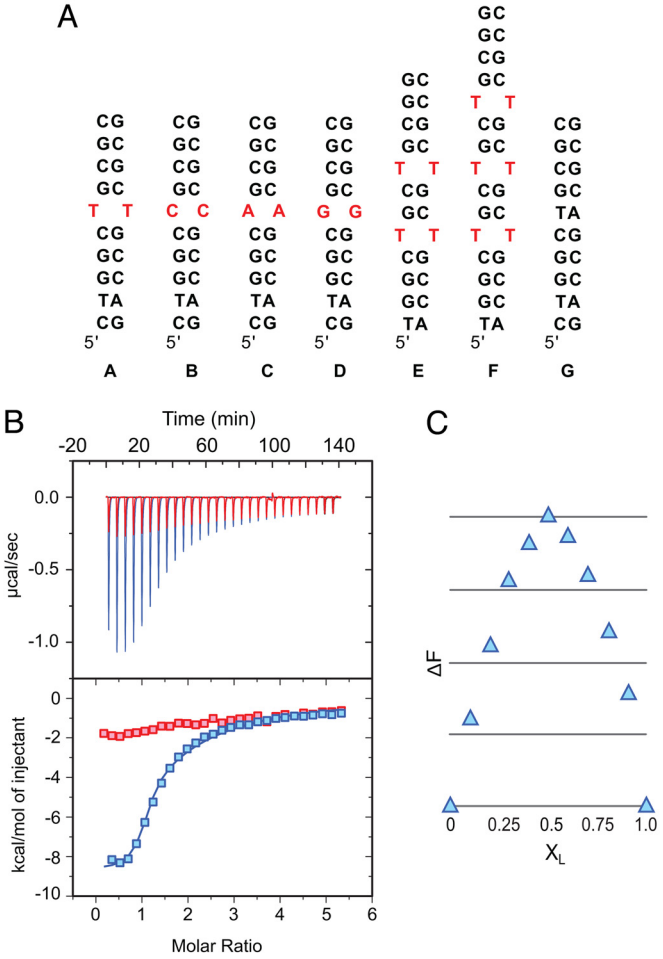

Fig. 3. (*A*) DNA duplexes studied by ITC. (*B*) ITC binding isotherm of 1 to sequence A (blue) and G (red). (*C*) Job plot analysis of 1 binding to step sequence A at a total concentration of 30 μM.

mismatch in comparison to the six hydrogen bonds predicted to be formed with a T-T or U-U mismatch. A small amount of heat generated in the ITC titration of **1** to duplex G (Fig. 3*B*) indicated binding but only a lower limit of K_d >100 μM could be assigned. Reverse titration experiments with fluorescence detection indicated minimal change in ligand fluorescence upon addition of G.

Table 1. Equilibrium dissociation constants* of ligand 1 to various nucleic acid secondary structures determined by ITC

Duplex/Hairpin	Target	K_d(1), μM	K_d(2), μM	K_d(3), μM
A	$d(CTG)_2$	0.39 ± 0.08	–	–
B	$d(CCG)_2$	5.0 ± 0.2	–	–
C	$d(CAG)_2$	66 ± 8.0	–	–
D	$d(CGG)_2$	33	–	–
E	$d(CTG)_4$	0.5 ± 0.2	10 ± 2	–
F	$d(CTG)_6$	0.5 ± 0.05	3.7 ± 0.6	18 ± 8
G	Duplex	>100	–	–
H	$r(CUG)_4$	0.43 ± 0.11	59 ± 20	–
I	$r(CUG)_2$	2.1 ± 0.2	–	–
J	$r(CCG)_2$	14 ± 2	–	–
K	$r(CAG)_2$	>300	–	–
L	$r(CGG)_2$	>300	–	–

*Average of 2–4 measurements. In cases where only 2 repeat experiments were made, no error is listed but the values were within 30%.

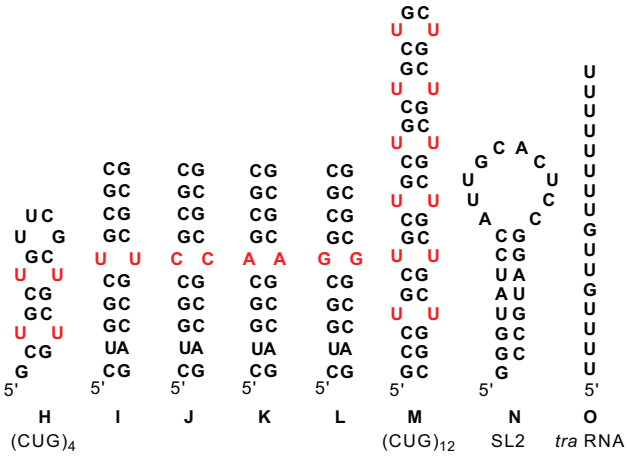

Fig. 4. RNA sequences used in inhibition assays, $(CUG)_4$, $(CUG)_{12}$, SL2 RNA, which is a target site for the U1A protein, and *tra* RNA, which is a target site for Sex lethal protein.

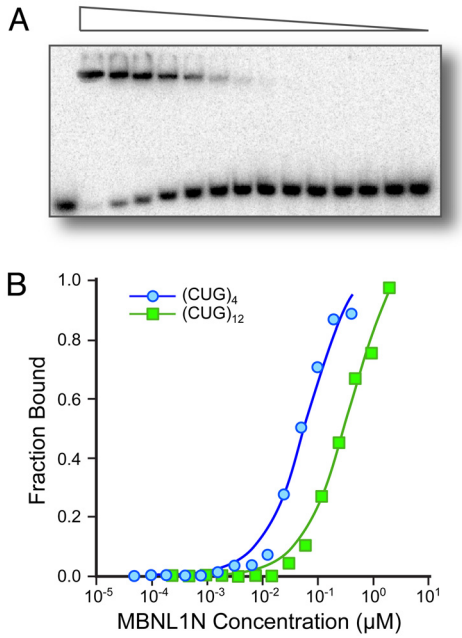

Fig. 5. (*A*) MBNL1N binding to $(CUG)_{12}$ in the presence of tRNA (0.9 μM) by gel mobility shift assay. The protein concentration ranges from 1.85 μM to 225 pM. (*B*) Plots illustrating the fraction of $(CUG)_4$ and $(CUG)_{12}$ RNAs bound as a function of MBNL1N concentration in the presence of 0.2 μM and 0.9 μM tRNA, respectively.

An intercalative mode of binding of **1** to DNA duplexes A and F was supported by two observations. First, ^{1}H NMR studies of the structure of **1** in water indicate an intramolecular π-stacked conformation (see *SI Appendix*). Second, an intercalative mode of binding of **1** to DNA duplexes A and F was suggested by circular dichroism (CD) studies. Thus, an increase in signal at 280 nm was observed in both cases, analogous to what has been reported for 9-aminoacridine intercalation in standard duplexes (16). No other major CD spectral changes were evident indicating little disruption of duplex structure due to ligand binding.

To examine the ability of **1** to bind multiple sites within a CTG repeat structure, sequences E and F were examined. ITC data using duplex E fit best to a sequential binding model with K_d values of 0.51 ± 0.15 and 10 ± 2 μM. This apparent negative cooperativity of neighboring T-T mismatches was confirmed by a 1.3:1 binding stoichiometry through Job analysis. A DNA sequence with two T-T mismatches separated by five GC base pairs showed 2:1 binding, indicating that the negative cooperativity requires proximity of the T-T mismatches (see *SI Appendix*). When the total concentration was increased 20-fold, 2:1 binding of **1** toward E became evident. The ITC data of 1 to sequence F provided K_d values of 0.47 ± 0.05, 3.7 ± 0.6, and 18 ± 8.0 μM with a Job analysis indicating 2:1 stoichiometry. Given the observed K_d values and the concentrations used for the Job analysis a 2:1 complex is expected. The two tightest binding sites exhibit K_d values that are 7.9-fold different possibly indicating some negative cooperativity through longer range communication between binding sites.

All of the data above were collected using DNA, a potential target for DM1 (*vide supra*) (1c,4). Importantly, the same affinity of **1** is evident toward the RNA sequence H, which contains the CUG repeat in an RNA stem-loop (17, 18). Thus, ITC indicated 1:1 stoichiometry and high affinity binding (K_d = 0.43 ± 0.11 μM), which was confirmed by reverse titration fluorescence (see *SI Appendix*). To determine whether the preference for the T-T mismatch seen in DNA is maintained in RNA, sequences I-L were studied (Fig. 4). The dissociation constants in these RNA duplexes are somewhat higher than those observed for DNA sequences A–D, but the analogous preference for U-U is observed (Table 1) with ligand **1** exhibiting a 6-, >143-, and >143-fold reduction in affinity toward single C-C, A-A, and G-G mismatches, respectively.

Given this encouraging result, the ability of **1** to destabilize the complex formed between poly(CUG)RNA and the protein MBNL1N was evaluated. The dissociation constants of complexes formed between MBNL1N and the $(CUG)_4$ and $(CUG)_{12}$ sequences, shown in Fig. 4, were determined to be 26 ± 4 nM and 165 ± 9 nM, respectively, using gel mobility shift assays (Fig. 5). Inhibition of complex formation was measured by titration of **1** into a constant concentration of the poly(CUG)RNA-MBNL1N complex. A representative inhibition assay and titration curve is shown in Fig. 6. The IC_{50} values and K_i values were similar for the $(CUG)_4$ RNA (IC_{50} = 52 ± 20 μM, K_i = 6 ± 2 μM) and $(CUG)_{12}$ RNA (IC_{50} = 46 ± 7 μM, K_i = 7 ± 1 μM). The binding and inhibition data are summarized in Table 2. The K_i value is ≈10-fold greater than the K_d values of **1** binding to $(CUG)_4$, which may be due to differences between the buffer conditions used in the two sets of experiments or may suggest that inhibition of the MBNL1N-$(CUG)_4$ complex requires binding of two molecules of **1** to the RNA.

The specificity of **1** for CUG RNA was further evaluated by measuring the ability of **1** to bind to tRNA and to inhibit the binding of MBNL1N to $(CUG)_4$ and $(CUG)_{12}$ RNAs in the presence of competitor tRNA. The affinity of **1** for tRNA was determined to be ≈10 μM by ITC, which is 23-fold weaker binding than **1** to $(CUG)_4$ RNA. The affinity of MBNL1N for $(CUG)_4$ and $(CUG)_{12}$ RNAs is reduced by 3- to 5-fold in the presence of tRNA (Table 2). Importantly, the IC_{50} and K_i values of **1** for $(CUG)_4$ or $(CUG)_{12}$ RNAs are changed only modestly, or not at all, by the addition of tRNA to the inhibition experiment (Table 2). As an additional evaluation of specificity, the destabilization of complexes formed between the RNA binding domains of the U1A and Sex lethal proteins and their cognate RNAs by **1** was investigated. Both U1A and Sex lethal protein use RNA recognition motifs (RRMs), which are unrelated to the zinc fingers of MBNL1N, to bind RNA. The target site for U1A is SL2 RNA a stem loop structure that does not contain any mismatched sequences, while the target site for Sex lethal is *tra* RNA, an unstructured single stranded U-rich sequence (Fig. 4). No destabilization of either complex was observed in the presence of **1** (see *SI Appendix*). Together, the results of these

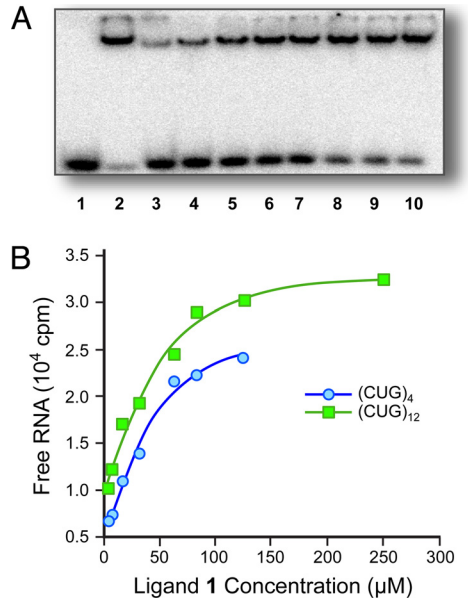

Fig. 6. (*A*) Inhibition of the MBNL1N-$(CUG)_{12}$ complex in the presence of tRNA (0.9 μM) with decreasing concentrations of ligand **1** in lanes 3–10: 250 μM, 125 μM, 83.3 μM, 62.5 μM, 31.3 μM, 15.6 μM, 7.8 μM, and 3.9 μM, respectively. Lane 1 is a control with only $(CUG)_{12}$ + tRNA, and lane 2 contains $(CUG)_{12}$ + MBNL1N complex in the presence of tRNA. (*B*) Plots illustrating inhibition of (CUG)n-MBNL1N complex with increasing concentrations of ligand **1**.

experiments are consistent with the specificity of **1** for DNA described earlier. Ligand **1** is specific for the CUG RNA in the presence of a large excess of competitor tRNA and does not destabilize RNA-protein complexes formed with RNAs that have some of the characteristics of the $(CUG)_n$ RNAs.

The mechanism by which **1** complexes RNA and disrupts the MBNL1N·RNA complex is not known. Nonetheless, the importance of the triaminotriazine unit and the four-methylene linker chain is apparent from a qualitative structure-activity relationship performed on the MBNL1N·$(CUG)_4$ complex using the gel-shift assay. Thus, **2** with a three-methylene linker is a less effective inhibitor, whereas **5** containing a 2-aminopyridine unit in place of the triazine unit and simple intercalators such as 6 and Actinomycin D exhibit minimal inhibition (see *SI Appendix*).

Conclusion

DM1 is a disease for which the most direct treatment at a molecular level can be envisioned to involve targeting the genetic DNA or the toxic mRNA transcript. The regular and repeating structures of the CUG repeats offer an opportunity for the rational design of specific inhibitors, which can prove to be a difficult approach for more varied and flexible RNA structures.

Table 2. Equilibrium dissociation constants for complexes formed between $(CUG)_4$ and $(CUG)_{12}$, and IC_{50}- and K_i values for inhibition of these complexes with 1 in the absence and presence of competitor tRNA

RNA	tRNA, μM	K_d, nM	[MBNL1N], μM	IC_{50}, μM	K_i, μM
$(CUG)_4$	—	26 ± 4	0.2	52 ± 20	6 ± 2
	0.2	70 ± 10	0.2	42 ± 20	11 ± 5
$(CUG)_{12}$	—	165 ± 9	0.925	46 ± 7	7 ± 1
	0.9	370 ± 20	0.925	43 ± 1	12.3 ± 0.3

Errors are the standard deviation of at least three independent measurements.

Indeed, the rational design approach that focused on a Janus wedge recognition unit to pair with the weakly hydrogen bonded U-U mismatch has yielded compound **1**, which is prepared in just two synthetic steps, binds with high nanomolar affinity to the target sites, and is selective in complexing both T-T and U-U mismatches. Specificity for the toxic RNA is essential for the development of therapeutic treatments using this approach, so that the small molecule does not inhibit MBNL1 binding to functional target sites. However, specificity is more difficult to achieve than high affinity. Thus, it is notable that compound **1** is selective for T-T and U-U mismatches over other mismatch pairs, indicating a sequence specificity that is unusual in RNA binding compounds. Compound **1** also shows high selectivity (>250-fold) for the CTG sequence relative to duplex DNA. As predicted from the binding experiments, low micromolar concentrations of ligand **1** destabilize complexes formed between toxic poly(CUG) sequences and MBNL1N even in the presence of competitor tRNA. Thus, ligand **1** is a potentially powerful lead compound for the development of molecules that could validate this approach and ultimately be used therapeutically.

To improve upon this lead compound, it will be important to gain more structural information. Of particular importance is determining the role of the Janus-wedge unit and whether the complexation occurs through the major or minor groove. Studies with compounds analogous to **1**, but lacking the triaminotriazine unit are both weaker binders and weaker inhibitors, which supports the Janus-wedge recognition model as the origin of the sequence selectivity, but other binding models are possible (see *SI Appendix*). If the stacked-intercalator model with U-U pairing by the triaminotriazine unit is indeed occurring, then further increases in selectivity and affinity might be achieved by replacing the flexible tether in **1** with a rigid linker that enforces the π-stacking and further weakens or prevents nonspecific DNA/RNA intercalation. A continued rational approach to improve specificity and affinity and an evaluation of the ability of **1** and related compounds to prevent formation of MBNL-poly(CUG) aggregates in cells are underway and will be reported in due course.

Materials and Methods

Compounds, Materials, and General Methods. All compounds described herein gave NMR and mass spectral data in accord with their structures, and each key compound gave a passing elemental analysis. The preparation of ligand **1** is representative and described below. The preparation of other compounds is described in the *SI Appendix* along with general methods used for their preparation and characterization. Details of the molecular modeling are also contained in the *SI Appendix*.

DNA oligomers were obtained from Integrated DNA Technologies and purified by standard desalting. Purified RNA sequences were obtained from Dharmacon Research. Yeast tRNA was purchased from Sigma-Aldrich.

***N*-(4-Aminobutyl)-[1,3,5]triazine-2,4,6-triamine 1a.** To 8.0 mL (79 mmol) of 4-diaminobutane in an oil bath at 130 °C was added 2.1 g (14 mmol) of 2,6-diamino-4-chloro-[1,3,5]triazine slowly over 30 min. The mixture was stirred for 1.5 h and then cooled to 80 °C. The excess diamine was removed in vacuo to produce a white solid. The solid was suspended in methanol (MeOH) and concentrated NH_4OH was added until the suspension became strongly alkaline. Solvent was removed under reduced pressure. The crude pellet was dissolved in CH_2Cl_2/MeOH and attached to silica and dry loaded for purification by column chromatography. Chromatography was performed with a solvent gradient from 10 to 20% MeOH in CH_2Cl_2 containing 2% NH_4OH to produce 2.27 g (11.5 mmol, 80%) of a white amorphous solid: ^{1}H NMR (500 MHz; DMSO-d_6) δ 7.89 (s, 2H), 6.48 (t, J = 5.8, 1H), 6.00 (d, J = 80.1, 4H), 3.18 (q, J = 6.1, 2H), 2.76 (t, J = 7.4, 2H), 1.51 (ddtd, J = 25.2, 15.6, 8.4, 7.1, 4H); ^{13}C NMR (125 MHz; DMSO-d_6) δ 167.2, 166.9, 166.3, 39.0, 38.6, 26.4, 24.4; *m/z* HRMS (ESI) calculated for $[M+H]^+$: 198.1467; found 198.1465.

***N*^{2}-(4-(6-Chloro-2-methoxyacridin-9-ylamino)butyl)-1,3,5-triazine-2,4,6-triamine (1).** To a refluxing suspension of 0.45 g (2.3 mmol) of **1a** and 0.77 g (2.3 mmol) of 6-chloro-2-methoxy-9-phenoxyacridine in 35 mL of freshly distilled aceto-

nitrile (MeCN) was added 35 drops of TFA. The reaction was stirred overnight at 90 °C allowing the product to form as a bright yellow precipitate. The suspension was cooled to ambient temperature, filtered, and washed with cold MeCN and Et_2O. Column chromatography with a solvent gradient from 10 to 20% MeOH in CH_2Cl_2 containing 2% NH_4OH to provided 1.1 g (1.74 mmol, 77%) of the TFA salt after acidification: mp 131–133 °C; ^{1}H NMR (400 MHz; DMSO-d_6) δ 13.77 (s, 2H), 9.60 (t, J = 5.7, 1H), 8.48 (d, J = 9.2, 1H), 8.14 (t, J = 5.1, 1H), 7.86–7.67 (m, 8H), 7.51 (d, J = 9.4, 1H), 4.09 (q, J = 6.4, 2H), 3.92 (s, 3H), 3.27 (q, J = 6.1, 2H), 1.88 (dt, J = 14.5, 7.4, 2H), 1.60 (dt, J = 14.5, 7.1, 2H); ^{13}C NMR (125 MHz; DMSO-d_6) δ 167.9, 167.7, 167.1, 155.7, 151.0, 148.9, 146.8, 134.0, 131.5, 127.9, 127.1, 124.9, 123.3, 117.7, 115.2, 101.3, 56.3, 50.0, 41.1, 28.8, 27.5; *m/z* HRMS (ESI) calculated for $[M+H]^+$: 439.1762; found 439.1747; Analytically calculated for $C_{21}H_{24}N_8OCl{\cdot}2TFA{\cdot}H_2O$: C, 43.84; H, 3.97; N, 16.36. Found: C, 44.00; H, 3.72; N, 15.75.

Abasic 1 ^{1}H NMR: (500 MHz; DMSO-d_6) δ 8.34 (d, J = 9.3, 1H), 7.87 (d, J = 2.2, 1H), 7.84 (d, J = 9.3, 1H), 7.61 (d, J = 2.6, 1H), 7.37 (ddd, J = 44.3, 9.3, 2.4, 2H), 6.91 (t, J = 6.1, 1H), 6.44 (t, J = 5.8, 1H), 5.96 (d, J = 69.2, 4H), 3.92 (s, 3H), 3.74 (q, J = 6.7, 2H), 3.15 (q, J = 6.4, 2H), 1.73 (dt, J = 14.6, 7.4, 2H), 1.51 (dt, J = 14.6, 7.2, 2H).

Thermal Denaturation Studies. Thermal denaturation studies were performed with a temperature controlled Shimadzu 2501PC UV-Vis recording spectrophotometer enabled with an eight-well quartz sample cell (1.0 cm path, 130 μL total volume). Stock solutions of 800 μM DNA oligomers were prepared, annealed in a water bath >90 °C for 5 min, and then allowed to cool to ambient temperature. One equivalent of the respective ligand was added, followed by 20 μL of 100 mM Mops pH 7.0, 10 μL of 3.0 M NaCl, and 10 μL of 10 mM EDTA. The samples were then diluted to 100 μL with water to give final concentrations of 12 μM DNA duplex, 12 μM ligand, 20 mM Mops pH 7.0, 300 mM NaCl, and 1.0 mM EDTA. Samples were then placed in the eight-well cell and cooled to 0 °C. The temperature dependent absorbance of each sample was monitored from 0 °C to 90 °C at 260 nm with a ramp rate of 1 °C per minute and monitoring every 0.5 °C. The melting temperature of each curve (inflection point of the sigmoidal transition) was determined by finding the maximum of the first derivative of the curve with Origin 7.0 (MicroCal).

Isothermal Titration Calorimetry. Isothermal titration calorimetry measurements were performed at 25 °C on a MicroCal VP-ITC (MicroCal). A standard experiment consisted of titrating 10 μL of a 500 μM ligand from a 250-μL syringe (rotating at 300 rpm) into a sample cell containing 1.42 mL of a 20 μM DNA/RNA solution. The duration of the injection was set to 24 s, and the delay between injections was 300 s. The initial delay before the first injection was 60 s. To derive the heat associated with each injection, the area under each isotherm (microcalories per second versus seconds) was determined by integration by the graphing program Origin 5.0 (MicroCal). The fitting requirements were such that the thermodynamic parameters were derived from curves that produced the lowest amount of deviation. In most cases, fitting to a sequential site binding model of two or three binding sites gave the most accurate data. In many cases, additional sites are not detected by Job plot analysis and likely represent low-affinity sites. Analogous low-affinity binding sites have previously been observed in aminoglycoside-16S rRNA interactions (19). The ligand stock solution was 10 mM in DMSO. The buffer solution for ITC experiments was 20 mM Mops, pH 7.0, 300 mM NaCl, and 5–10% DMSO to balance the residual DMSO in the ligand solution.

Fluorescence Experiments. Fluorescence binding experiments and Job plot analysis were performed using a temperature controlled Horiba Jobin Yvon fluorimeter with a 250 μL cell with a 0.1-cm path.

Fluorescence Binding Experiments. A cell sample (250 μL) of 0.2 μM **1** (in 20 mM Mops, pH 7.0, 300 mM NaCl) was excited at 310 nm (excitation slit of 4 nm) and emission recorded between 470–530 nm (emission slit of 8 nm), monitoring the maximum at 495 nm. A concentrated sample of freshly annealed DNA/RNA was added as 1-μL injections via pipette. The sample was then allowed to equilibrate for 15 min, and the fluorescence emission recorded. The decrease in fluorescence with increased DNA/RNA was monitored until the binding sites became saturated and the fluorescence change was no longer evident. Preparation of concentrated DNA/RNA samples: the DNA/RNA duplex (400 μM) was heated in a water bath (>90 °C) for 5 min and then allowed to re-anneal by slowly cooling to ambient temperature. DNA/RNA samples ranging from 400–25 μM were prepared by serial dilution.

The percentage bound ($F\text{-}F_o/F_f\text{-}F_o$) versus [DNA/RNA] was plotted and fit to the one binding site model:

$$y = (a \times x)/(K_d + x)$$

where *a* is the asymptotic limit. Experiments were performed in triplicate.

Job Plot Analysis. Stock solutions of both ligand and nucleic acid duplex were prepared in equal concentrations with 20 mM Mops, pH 7.0, and 300 mM NaCl. The DNA/RNA duplexes were annealed as previously described. Samples of varying molar ratios of ligand:DNA/RNA were prepared while the total concentration remains constant. The fluorescence of each sample was recorded in addition a control sample containing only the ligand. Plots of ΔF versus molar ratio were produced to determine binding stoichiometry of 1:1 or 2:1.

Protein Expression and Purification. An expression vector for MBNL1N (1–272 aminoacids) was obtained from Maurice S. Swanson (University of Florida, College of Medicine, Gainesville, FL). MBNL1N is comprised of the four zinc finger motifs of MBNL1 and contains a hexahis tag. The protein was expressed and purified as described previously (20). The molecular weight was confirmed by MALDI mass spectrometry and the concentration was determined by amino acid analysis.

Equilibrium Binding Assays. RNA was labeled with [γ-^{32}P]ATP using T4 polynucleotide kinase (New England Biolabs). Labeled RNA (5 μL, 5 nM) was heated at 95 °C for 2 min and then placed on ice for 10 min and diluted to 125 μL in RNA storage buffer [66 mM NaCl, 6.7 mM $MgCl_2$, and 27 mM Tris·HCl (pH 7.5)]. If required for the experiment, tRNA was added to the RNA solution to give a final concentration of approximately 8 μM. The protein (MBNL1N) was serially diluted in binding buffer [175 mM NaCl, 5 mM $MgCl_2$, 20 mM Tris·HCl (pH 7.5), 1.25 mM BME, 12.5% glycerol, 2 mg/mL BSA, and 0.1 mg/mL heparin], and 5 μL of protein solution was added to 5 μL of RNA solution (17). The reaction mixture was incubated at room temperature for 25 min and loaded onto a 6% polyacrylamide gel (80:1) at 4 °C. The gels were run for 1 h at 360V in 22.5 mM Tris-borate buffer (pH 8). Gels were visualized on a Molecular Dynamics Storm phosphorimager. The apparent K_d values were obtained by fitting fraction RNA bound versus protein concentration using the following equation: fraction bound = $1/(1+(K_d/[P]_T))$. All binding measurements were performed with a greater than 10-fold excess of protein over RNA in each binding reaction used to determine the K_d so that [P] would be approximately equal to $[P]_{total}$.

Inhibition Assays. The inhibition of the MBNL1N-RNA complex was investigated using the above procedure except that the small molecule was added to the RNA-protein complex after 25 min of incubation. The reaction mixture was incubated for an additional 10–15 min at room temperature. The inhibition assays were performed in the presence of 10% DMSO. To determine IC_{50} values, the free RNA versus small molecule concentration was fit to the equation: $B = \Delta B \exp((-0.69/IC_{50})C) + B_f$. B is the volume of the free RNA band in the gel, ΔB is the difference between the volumes of the free RNA bands at the lowest and highest concentrations of small molecule (B_i-B_f), C is the concentration of the small molecule, and IC_{50} is the concentration of small molecule at which $B = (1/2\Delta B) + B_f$. The apparent inhibition constant (K_i) was determined using the equation: $K_i = IC_{50}/(1+([P]_T/K_d)$, where $[P]_T$ is the total concentration of protein and K_d is the dissociation constant of the MBNL1N-RNA complex.

U1A and Sex lethal proteins were expressed as hexa-his constructs and were purified using a Ni-NTA column from Qiagen. For U1A, inhibition assays were performed as reported previously for gel shift binding assays with 20 nM U1A (21). The K_d of the U1A-SL2 RNA complex under these conditions is 0.5 nM. For Sex lethal, inhibition assays were performed in 15 mM HEPES, pH 7.6, 50 mM potassium chloride, 1 mM EDTA, 1 mM β-mercaptoethanol, 20% glycerol, and 0.005% Triton-X, with 0.2 μg/μL t-RNA with 250 nM Sex lethal protein and 0.2 nM ^{32}P-labeled *tra* RNA. Under these conditions, the K_d of the Sex lethal-*tra* RNA complex is 70 nM.

ACKNOWLEDGMENTS. This work was supported by the National Institutes of Health and the National Science Foundation.

1. de León MB, Cisneros B (2008) Myotonic dystrophy 1 in the nervous system: From the clinic to molecular mechanisms. *J Neurosci Res* 86:18–26.
2. Mirkin SM (2007) Expandable DNA repeats and human disease. *Nature* 447:932–940.
3. Miller JW, et al. (2000) Recruitment of human muscleblind proteins to (CUG)(n) expansions associated with myotonic dystrophy. *EMBO J* 19:4439–4448.
4. Mooers BHM, Logue JS, Berglund JA (2005) The structural basis of myotonic dystrophy from the crystal structure of CUG repeats. *Proc Natl Acad Sci USA* 102:16626–16631.
5. Hagihara M, Nakatani K (2006) Inhibition of DNA replication by a d(CAG) repeat binding ligand. *Nucleic Acids Symp Ser* 50:147–148.

6. Nakatani K, Sando S, Kumasawa H, Kikuchi J, Saito I (2001) Recognition of guanine-guanine mismatches by the dimeric form of 2-amino-1,8-naphthyridine. *J Am Chem Soc* 123:12650–12657.
7. Kobori A, Horie S, Suda H, Saito I, Nakatani K (2004) The SPR sensor detecting cytosine-cytosine mismatches. *J Am Chem Soc* 126:557–562.
8. Li XH, Song HF, Nakatani K, Kraatz HB (2007) Exploiting small molecule binding to DNA for the detection of single-nucleotide mismatches and their base environment. *Anal Chem* 79:2552–2555.
9. Lian CY, Robinson H, Wang AHJ (1996) Structure of actinomycin D bound with (GAAGCTTC)(2) and (GATGCTTC)(2) and its binding to the (CAG)(n) :(CTG)(n) triplet sequence as determined by NMR analysis. *J Am Chem Soc* 118:8791–8801.
10. David A, et al. (2003) DNA mismatch-specific base flipping by a bisacridine macrocycle. *Chembiochem* 4:1326–1331.
11. Gareiss PC, et al. (2008) Dynamic combinatorial selection of molecules capable of inhibiting the (CUG) repeat RNA-MBNL1 interaction in vitro: Discovery of lead compounds targeting myotonic dystrophy (DM1). *J Am Chem Soc* 130:16254–16261.
12. Branda N, Kurz G, Lehn JM (1996) Janus Wedges: A new approach towards nucleobase-pair recognition. *Chem Commun* 21:2443–2444.
13. Chen H, Meena, McLaughlin LW (2008) A Janus-Wedge DNA triplex with A-W-1-T and G-W-2-C base triplets. *J Am Chem Soc* 130:13190–13191.
14. Constant JF, Laûgaa P, Roques BP, Lhomme J (1988) Heterodimeric molecules including nucleic-acid bases and 9-aminoacridine—Spectroscopic studies, conformations, and interactions with DNA. *Biochemistry* 27:3997–4003.
15. Rojsitthisak P, Romero RM, Haworth IS (2001) Extrahelical cytosine bases in DNA duplexes containing d[GCC](n) d[GCC](n) repeats: Detection by a mechlorethamine crosslinking reaction. *Nucleic Acids Res* 29:4716–4723.
16. Eriksson M, Norden B (2001) Linear and circular dichroism of drug-nucleic acid complexes. *Methods Enzymol* 340:68–98.
17. Warf MB, Berglund JA (2007) MBNL binds similar RNA structures in the CUG repeats of myotonic dystrophy and its pre-mRNA substrate cardiac troponin T. *RNA* 13:2238–2251.
18. Molinaro M, Tinoco I (1995) Use of ultra-stable UNCG tetraloop hairpins to fold RNA structures—Thermodynamic and spectroscopic applications. *Nucleic Acids Res* 23:3056–3063.
19. Kaul M, Pilch DS (2002) Thermodynamics of aminoglycoside-rRNA recognition: The binding of neomycin-class aminoglycosides to the A site of 16S rRNA. *Biochemistry* 41:7695–7706.
20. Yuan Y, et al. (2007) Muscleblind-like 1 interacts with RNA hairpins in splicing target and pathogenic RNAs. *Nucleic Acids Res* 35:5474–5486.
21. Shiels JC, Tuite JB, Nolan SJ, Baranger AM (2002) Investigation of a conserved stacking interaction in target site recognition by the U1A protein. *Nucleic Acids Res* 30:550–558.